Arch. Mech., 35, 4, pp. 475-489, Warszawa 1983

Temperature determination in dynamic plasticity by infrared radiation detection

M. MALATYŃSKI, W. K. NOWACKI and W. OLIFERUK (WARSZAWA)

THE OBJECT of the work is to measure the temperature and the deformation field in solids (e. g. aluminium) during its dynamic plastic strain at higher strain rates. The present paper describes the testing stand based on a Hopkinson pressure bar system and AGA 680 thermovision set; details of the experiment; analysis of the experimental results and their comparison with the theoretical and numerical results presented in [1].

Przedmiotem pracy jest pomiar pola temperatury i odkształcenia w ciałach stałych (na przykładzie próbek aluminiowych) w procesie ich dynamicznego plastycznego odkształcenia z dużymi prędkościami odkształcenia. W pracy opisano stanowisko badawcze składające się z układu prętów Hopkinsona i układu termowizyjnego AGA 680; szczegóły doświadczenia, analizę wyników doświadczalnych oraz ich porównanie z wynikami teoretycznymi (rozwiązaniami numerycznymi) przedstawionymi w pracy [1].

Предметом работы является измерение поля температуры и деформации в твердых телах (на примере алюминиевых образцов) в процессе их динамической пластической деформации с большими скоростями деформаций. В работе описаны исследовательская установка, состоящая из системы стержней Гопкинсона и термовизионной системы АГА 680, подробности эксперимента, анализ экспериментальных результатов и их сравнение с теоретическими результатами (численнными решениями), представленными в работе [1].

Introduction

THE OBJECT of the present work is to measure the temperature field of a material during its dynamic plastic strain at higher strain rates of the order 10^2–10^4 s^{-1}. This range of strain rate is possible only in compression tests. Special measuring techniques and signal amplifying and recording apparatus with wide passing bands are used in this kind of experiments.

In the recent fifteen years a considerable advance has been made in experimental investigations of the mechanical properties of metals which are subject to widely varying strain rates and temperatures. These investigations were intended to provide data for the formulation of constitutive equations that would be valid for a large range of temperatures and different types of loadings, namely: monotonous, cyclic, static, dynamic, uniaxial and complex. Such experiments are conducted usually at a constant temperature either in a controlled atmosphere or in vacuum. A survey of these experimental works is given in [9] by P. PERZYNA and for steel in [8] by other authors.

The first papers on the determination of temperature variation in solids due to their dynamic deformation were published a few years ago. This beginning coincided with the appearance on the market of infrared cameras which were sufficiently sensitive to record

temperature variations smaller than 0.2°C. Literature in this field has been scarce so far. It is possible to quote here some interesting works on fracture mechanics [4], vibration mechanics [10], solid mechanics [5], and on the determination of the energy stored in tensioned metal [6]. The experiments were carried out with the help of thermovision apparatus which utilizes the effect of infrared radiation emission by all materials at temperatures higher than absolute zero. The power of this radiation obeys the Stefan–Boltzman law and thus it is a unique function of the temperature of the emitting surface. Thermovision apparatus is capable of recording the distribution of the radiation emitted from the surface. The radiation is scanned from the emitting surface by the optical system of the thermovision camera and then it is focussed on the detector which converts infra-red radiation into a proportional electric signal. This kind of detector enables further processing of the signal obtained. For instance, after amplification it can be used to modulate the electron beam in the image tube which displays the distribution of the power of the infra-red radiation emitted by the surface. The measured signal of distribution can be processed in such a way as to obtain the relevant temperature distribution. No inertial effect is virtually involved in the temperature measurement based on the detection of infra-red radiation. Moreover, the measuring system has no contact with the sample and this is an important advantage, particularly in dynamic tests.

The present work describes the testing stand, details of the experiment, analysis of the measuring results and their comparison with the theoretical discussion presented in [1].

1. Description of the test stand

The test stand is based on a modified Hopkinson pressure bar [3] system and AGA 680 thermovision set. It is designed for dynamic compression of cylindrical samples and for thermovision recording of the temperature distribution.

The Hopkinson pressure bar system consists of a compressed-air gun *1* and its tube (Fig. 1), a set of bars *3* and *4* and a dash-pot *6*. The tested sample *2* leaves the gun tube at a high velocity, it strikes against the face of bar *3* and becomes considerably deformed. The sample velocity is measured by means of laser *9*, the beam of which is split by a set of prisms *10* into two parallel beams directed towards phototransistors *8*. When the first laser beam is cut off by the striker sample, the phototransistor produces an electric signal actuating a timer counter *11* which is stopped at the instant when the striker sample cuts off the second beam.

A compressive elastic wave with an amplitude of $-\varepsilon_i$ is produced in the measuring bar by the impact of the cylindrical sample. This wave arrives at the other end of the bar and travels back in this bar as an extensile elastic wave having an amplitude of $-\varepsilon_r$. A potentiometric strain gauge system is mounted at the mid-length of the impacted bar. Its signal is processed in amplifier *17* and recorded in one of the channels of a digital storage oscilloscope. This signal represents the initial and reflected compression elastic waves as functions of time. The oscilloscope time base is triggered by another potentiometric strain gauge system fixed at the front part of the bar. With such an arrangement it is

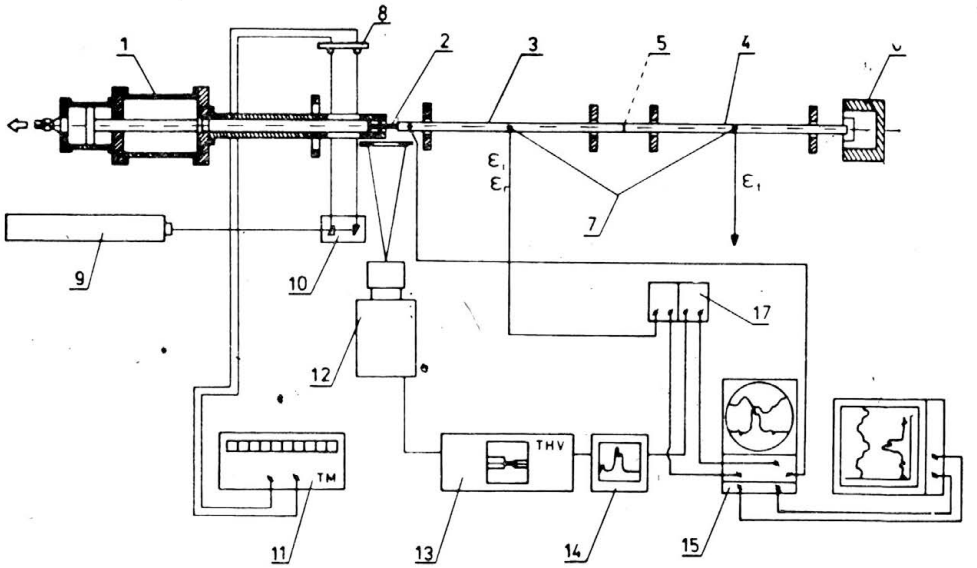

FIG. 1. Schematic diagram of experimental stand for dynamic compression of cylindrical samples with thermovision temperature recording.

possible to obtain a "waiting" time base and to record the full shapes of the initial and reflected waves, and to establish a fixed reference point on the time axis.

The impact point of the sample as it is striking against the active measuring bar is observed by a camera *12* of the AGA 680 thermovision set. The camera is located at a distance of 300 mm from the geometric axis of the bars and the gun tube so as to take a sharp image in the detector plane. The sample is deformed for a period which is too short to enable the accompanying increase of temperature to be observed as a thermovision image on *13*. The temperature variation discussed is determined by analysing the amplified detector signal produced by the infrared radiation emitted from the sample surface points which lie on the line parallel to the axis of the sample, that is, by analysing the signal of the thermovision image line. This signal is observed on the screen of an oscilloscope attachment and recorded on the screen of the digital oscilloscope.

The two-channel digital storing oscilloscope is capable of permanently recording (storing) electric signals fed at the instant of triggering the time base. In this way it is possible, at the instant at which the sample gives an impact to the bar, to record simultaneously (in channel No 1) the elastic wave propagating in the bar and (in channel No 2) the distribution of infrared radiation power along the sample axis. If the sample surface emission is homogeneous, then the distribution of infrared radiation power is proportional to the temperature distribution.

2. Description of experiments

Two kinds of experiments were performed. The first kind involved an impact of a long cylindrical sample given transmitted to a bar system. In the second kind, a slim cylindrical

ample was dynamically deformed in the classical system of a Hopkinson bar, the sample being sandwiched between two bars, one of which was subject to impacts of the steel striker bar.

2.1. Preparation of samples

The samples were made of a soft aluminium alloy PA1. In the first experimental version, the cylindrical samples were $d_0 \approx 9.80$ mm in diameter and $l_0 \approx 95$ mm in length. The carrying part was limited by two teflon rings $L_f = 3$ mm thick. The rings were intended to ensure the coaxial motion of the sample inside the gun tube. The sample had no side contact during its motion inside the gun tube. Thus it was possible to avoid any friction effect and related heat as well as misinterpretation of the measurement results. Circumferential lines parallel to the sample face were marked every 5 mm on the cylindrical surface in order to measure the permanent longitudinal deformations.

In the second experimental version, the samples made of PA1 alloy had the shape of a short cylinder (disc) which was $d_0 = 10$ mm in diameter and $l_0 = 5$ mm in length. The cylindrical surfaces of both types of the samples were coated with soot to improve the emission of heat and thus to obtain more intense signals which were displayed as thermovision images on the monitor screen. The faces of the cylindrical samples were coated with a thin layer of a high quality grease.

2.2. Calibration of temperature measuring system

The signal at the detector output is a function of the difference of temperatures of the sample under test and that existing in its nearest neighbourhood. Temperature of this region varies in an uncontrolled way and thus impedes the measurement of the sample temperature. To solve this problem, an indicator of constant temperature was placed in the viewing field of the camera. This was a segment of a resistance wire fed with stabilized current. With such an arrangement, every recording of the temperature distribution on the sample transmitting an impact to the bar was preceded by a maximum, the source of which was the radiation emitted by the wire having a constant unknown temperature. This constant temperature played the role of a constant reference level. To find the relation between the temperature of the sample and the power of radiation emitted, that is, to determine its absolute temperature, the sample was replaced by a small tank connected with a temperature-controlling ultrathermostat. The temperatures of the tank surface and the water contained in the ultrathermostat may differ from each other even at a steady thermal state. For this reason a thermocouple was installed to measure the temperature of the tank surface. The side tank surface, made of the same material as the sample, was blackened only to half of its length as measured along the tank axis. This was intended to determine the emissivity versus temperature for both the bright and blackened surfaces. The measurement results are shown in Fig. 2 in the form of two diagrams $T = f(H_c/H_w)$ and $T = f(H_b/H_w)$, where H — value of the maximum of temperature distribution recorded in the thermovision system, while the indices w, b and c denote the indicator, white (natural) and blackened surfaces, respectively. The thermocouple was calibrated

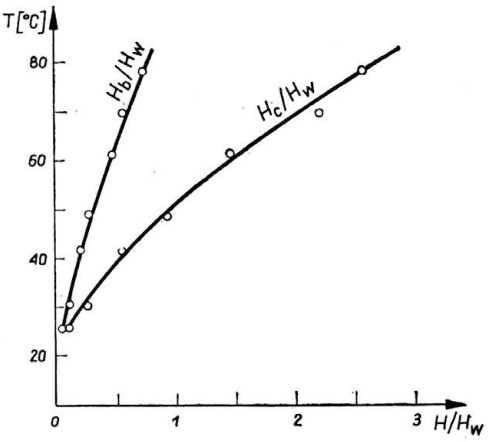

FIG. 2. Temperature versus ratio of infrared radiation power of aluminium tank; H — maximum of temperature distribution recorded by thermovision system (indices w, b and c denote indicator, white surface and black surface, respectively).

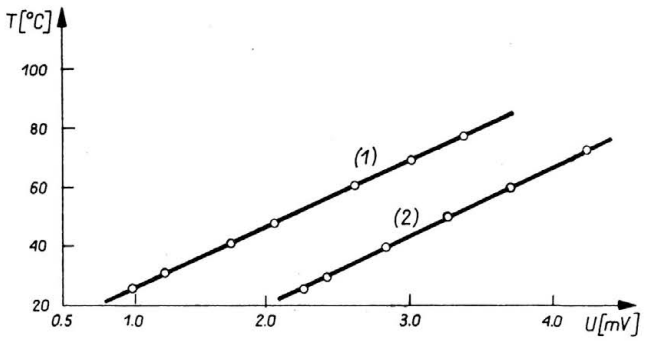

FIG. 3. Temperature versus voltage across ther mocouple: *1* — temperature of liquid flowing through tank, *2* — temperature of tank placed in ultrathermostat.

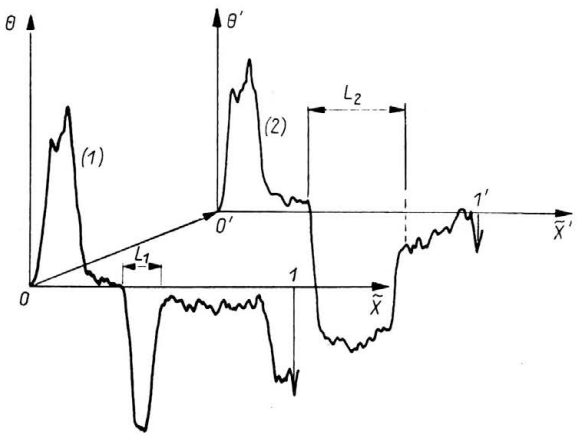

FIG. 4. Records of thermographic image of the heated bar ends, *1* — distance between pressure bars L_1, *2* — distance between pressure bars L_2.

by placing it together with the small tank into the ultrathermostat. The obtained diagrams $T = f(U)$, where U — voltage across the thermocouple terminals, are almost linear in both cases: when water was supplied to the tank from the ultrathermostat and when the thermocouple and tank were placed into the ultrathermostat (cf. Fig. 3). To ascribe the measured temperature distribution to concrete physical objects (sample, impacted bar), the thermographic image of the slightly heated bar end was recorded in two positions, namely: in the working position, and as the bar protruding at a known length (Fig. 4). The thermographic image of the bar and the indicator located at a fixed position enable to ascribe the recorded quantities to the physical configurations of the objects at the point of their impact.

2.3. Impact between long cylindrical sample and rigid obstacle

Two sequences of tests involved 20 and 10 samples, respectively. Argon was pumped into the gun chambers at pressures ranging from 4 to 8 atm to attain impact velocities of the sample of 50 to 150 ms^{-1}. For the given impact velocities, the sensitivities of the thermovision system adjusted by trials were 20 and 100 for white (natural) and blackened samples, respectively. With a signal division of 20, the sensitivity of the thermovision system is 5 times that corresponding to a division of 100. The sensitivity of the numerical oscilloscope was virtually constant. It was 0.1 mV per graduation in the channel used to record the sample radiation power distribution during impact, and 0.5 or 0.2 mV per graduation in the channel recording the elastic wave in the bar. The oscilloscope time base was 0.1 ms/cm.

2.4. Experiments with modified Hopkinson bar system [3] performed on short cylindrical samples

The short cylindrical samples were tested by means of a modified Hopkinson bar system described in detail in [3]. The thermovision camera was located at a distance from the geometrical axis of the sample sandwiched between two bars. The contacting faces of the sample were coated with grease, while the cylindrical surface had its natural colour. The sample was dynamically deformed by the striker bar of 200 mm in length and 20 mm in diameter which gave an impact to the incident bar. Since the mass of the striker bar was rather large, the gun was filled with gas under a pressure of $p = 3$ to 4 atm and thus it was possible to attain impact velocities from 6 ms^{-1} to 23 ms^{-1}. The system consisting of a digital oscilloscope and a $x-y$ plotter recorded the power of the infrared radiation emitted by the cylindrical sample surface and the elastic wave propagating in the incident bar. The wave propagating in the third bar was not recorded. The oscilloscope channel sensitivity and time base were adjusted to the same level as for the tests on long cylindrical samples. The sensitivity of the thermovision system was 20.

3. Experimental results

3.1. Impact between striking sample and bar

The results of each test performed on a long cylindrical sample are presented on the common diagram of the elastic wave $\varepsilon(t)$ propagating in the impacted bar and the radiation

power distribution $\theta(t)$ within the thermovision camera observation field embracing the indicator, sample and bar face (Fig. 5 and Fig. 8). These testing results were taken from the digital oscilloscope. The elastic wave consists of sequences of compressive and extensile waves. Their shapes can be approximated by means of trapezoids with superimposed disturbances. The power of the radiation observed by the camera varies both in time

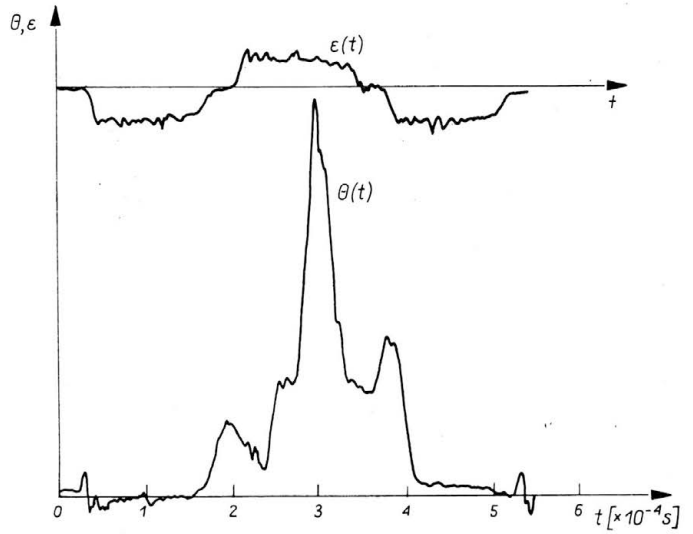

FIG. 5. Elastic wave travelling through impacted bar $\varepsilon(t)$ and radiation power distribution $\theta(t)$ in the observation field of thermovision camera.

and space. The principle of operation of the thermovision camera used in the present experiments consists in observing the successive points of a selected sample line by means of a rotating prism. After an observation cycle of a $L_c = 7.056$ cm long line from the left to the right side during the time period of $\Delta t_T = 5.56 \cdot 10^{-4}$ s, the prism jumps, in a time period of $\Delta t'_T = 8.8 \cdot 10^{-6}$ s, to the next observation cycle. The principle of operation of the thermovision camera used in the present tests is illustrated in Fig. 6. It is a plot of (X, t) and the origin of the coordinate system is located at the bar boundary. The dashed ordinate lines enclose the observation range of the thermovision camera, while the couples of heavy lines correspond to the cycles $m = 0, 1, 2, 3, \ldots, k$ during which the strong discontinuity wave propagates through the sample; the straight lines $n = 0, 1, 2, 3, \ldots, l$ determine the points of surface (X, t) at which the power of the radiation emitted by the sample is recorded. Since the camera is not triggered at the instant of impact but operates continuously, it observes, at the beginning of the impact, an arbitrary point located at the length L_c. Thus it completes this observation cycle and, say at an instant t_0, it starts a new full record of the radiation power of the entire line L_c. It is possible to record the infrared radiation of the sample surface on its meridian line as a function of time. Radiation is recorded on line $X_1 = v_{\text{cam}}(t - t_D)$ (Fig. 7), where v_{cam} is the "sweeping velocity" of the camera along a selected horizontal line corresponding to the meridian line of the cylindrical sample. Figure 7 illustrates the wave propagating in the sample

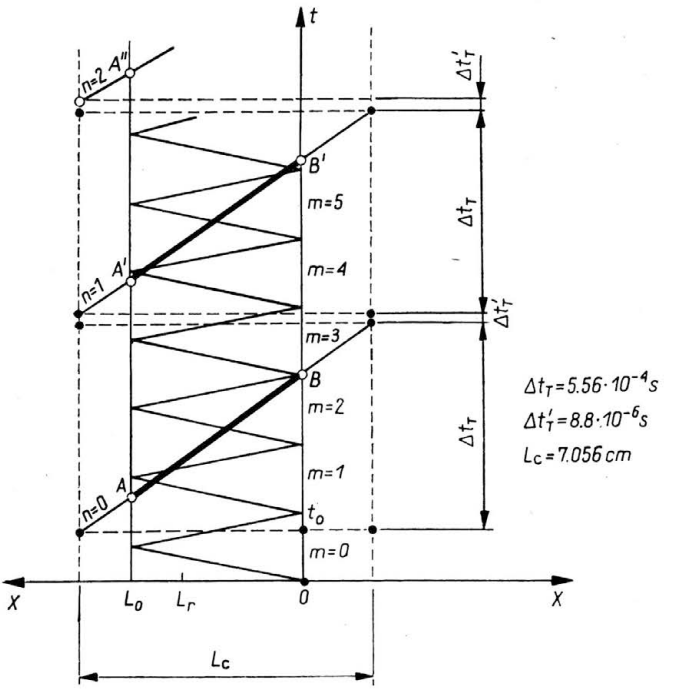

FIG. 6. Schematic diagram of images recorded by thermovision camera.

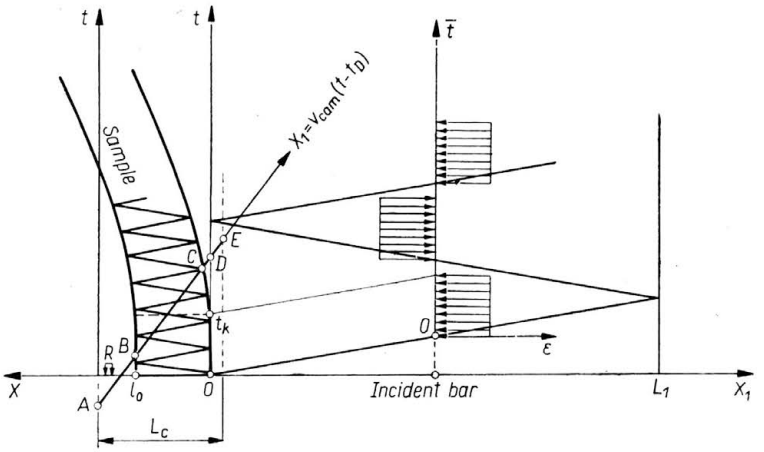

FIG. 7. Images of waves propagating in sample and incident bar. Infrared radiation power is recorded on line *AE*.

and the incident bar on the phase plane (X, t). Points A, B, C, D, E and R correspond to the points shown in Fig. 8. The sample looses its contact with the bar at instant t_k.

On the diagram $\theta(X_1)$ (Fig. 9), a complete observation cycle is contained between two points at which the observed quantity changes its sign. On the same diagram prepared for a striker velocity of $v \approx 100\ \mathrm{ms}^{-1}$ and for blackened surface (its emission is approxi-

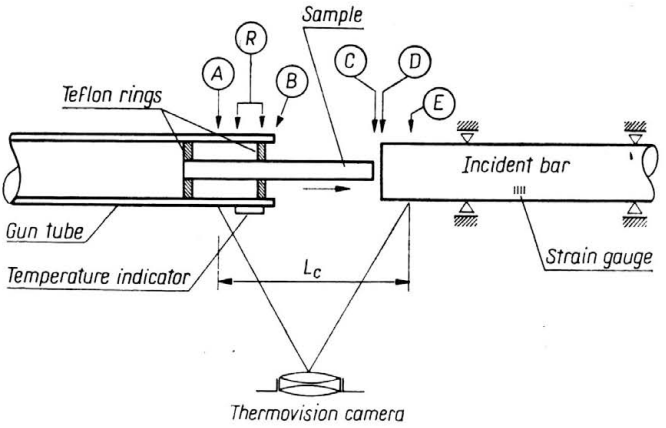

FIG. 8. Observation field of thermovision camera.

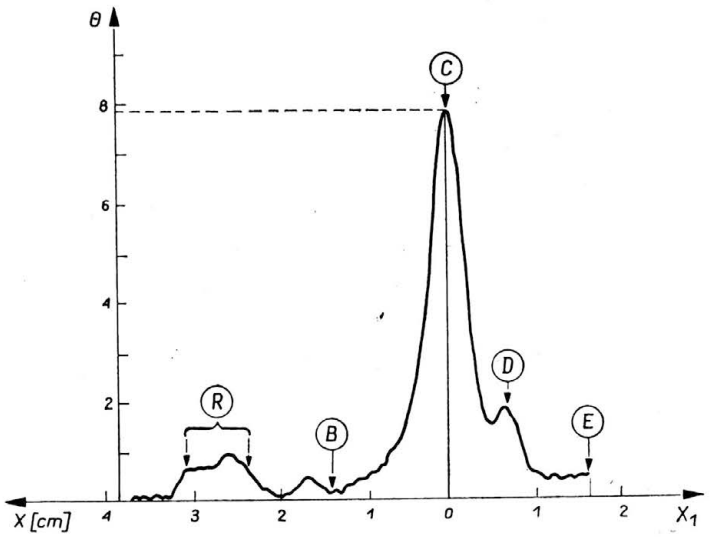

FIG. 9. Typical curve of sample radiation power versus X_1.

mately 5 times that of natural colour), it is possible to distinguish three maxima (Fig. 9). The first maximum (rather weak) located at the left side is caused by the heat radiation of the indicator heater wires (point *R*); the second maximum (most clear at point *C*) and the third maximum (at point *D*) correspond to the end of the striker bar and the end of the incident bar, respectively, both ends being heated up during the impact. The obtained results for both series of the samples are reproducible. By changing the frequency of the oscilloscope time base, it is possible to take records of two more time sequences of radiation power at the impact point by means of the camera sweeping from the left to the right side. Specimen records of four successive sequences starting every $\Delta t_T + \Delta t'_T = 5.65 \cdot 10^{-4}$ s are given in Fig. 10. The first maxima were not displayed completely on the oscilloscope

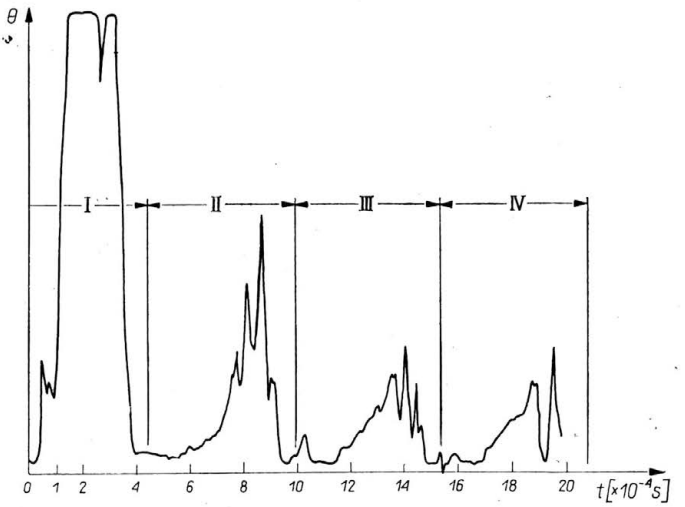

FIG. 10.

screen: successive sequences, numbers 2 and 3, are of similar shapes but their maxima are lower. The temperature drops abruptly because much heat is released from the ends of the bar and sample through conduction and radiation. From the records of deformation $\varepsilon(t)$ in the incident bar (cf. Fig. 5), it is possible to determine the strain and stress at the contact point of the sample and the bar (under the assumption that the incident bar is elastic). The contact period t_k can also be determined. Permanent longitudinal and transverse deformations Δ_{11} and Δ_{22} were measured.

3.2. Experimental results with the modified pressure Hopkinson bar

In comparison with the test involving an impact against an elastic obstacle, the present experiments differ only in the sample shape and in the way of producing the plastic deformation. The long sample ejected from the gun tube was replaced by a thin cylindrical sample sandwiched between two elastic bars and deformed by the third bar striking them. No changes were introduced into the system that recorded the same physical quantities. Similarly as in the preceding case, the two-channel oscilloscope recorded two varying quantities, namely: the power of radiation emitted by the cylindrical sample surface (line) and the wave $\varepsilon_i(t)$ travelling in the incident bar. No third channel was available to record the wave $\varepsilon_t(t)$ which passes through the deformed sample and is transmitted through the second impacted bar.

Figure 11 shows the quantities $\theta(t)$ and $\varepsilon_i(t)$ taken from the oscilloscope screw for sample 5D. The compressive wave $\varepsilon_i(t)$ and extensile wave $\varepsilon_r(t)$ reflected from the sample face can be approximated by trapezoidal figures. Thus it is possible to calibrate the system dynamically so that the maximum deformation corresponding to the wave $(\varepsilon)_{\max} = v_{\text{str}}/2c_0$ can be found from the measurement of the striker impact velocity v_{str}. In this way one can determine the direct relation between mechanical quantities (deformation) and electrical quantities, i.e. the signals fed from strain gauges and recorded on the diagram. The dis-

tribution pattern of the power of infra-red radiation recorded by the thermovision system is also qualitatively similar. The initial velocity of the striker bar is restricted by the strength of the remaining bars used in the experiment. Due to low initial velocity and small mass of the sample, the power of the radiation emitted is much lower than that produced by the heater wires of the indicator. Thus the distribution pattern of radiation power correspon-

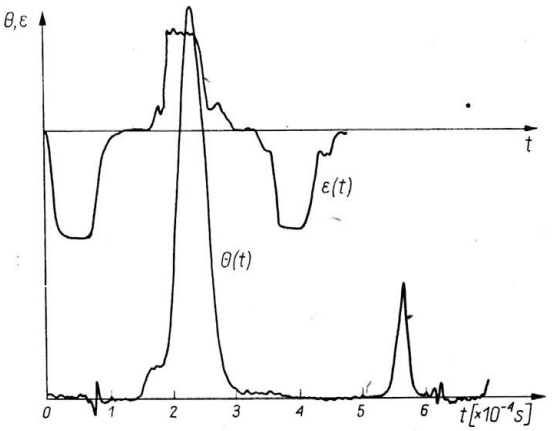

FIG. 11. Deformation $\varepsilon(t)$ in Hopkinson pressure bar and sample surface radiation power $\theta(t)$.

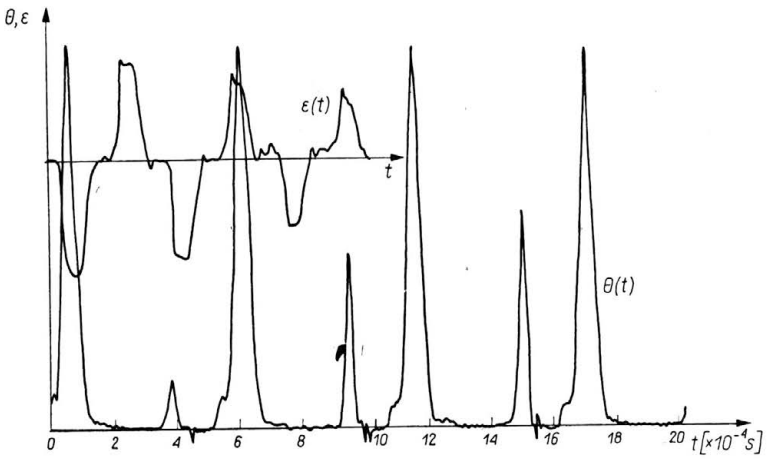

FIG. 12. Deformation $\varepsilon(t)$ in Hopkinson pressure bar and sample surface radiation power $\theta(t)$.

ding to a single observation camera sequence consists of a clear peak (indicator) and a single, much lower maximum produced by the sample radiation.

Figure 12 shows the experimental results obtained for sample 9*D*. By doubling the time base period it was possible to record three successive sequences of radiation of the sample during deformation. By applying a longer period of time base, as many as eight successive sequences of radiation power were recorded for sample 7*D* (see Fig. 13).

It is seen from these diagrams that, with a striker impact velocity of $v_{str} \approx 20$ m/s, the sample temperature increases for about 2.10^{-3} s (three successive sequences) and for about 3.10^{-3} s it remains approximately constant.

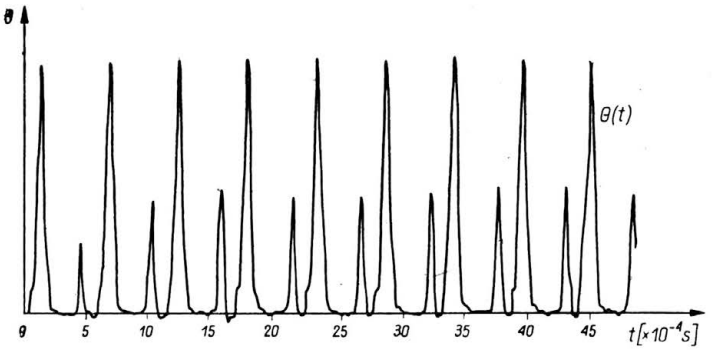

FIG. 13. Effect of double extension of oscilloscope time base as compared to image recorded in Fig. 12.

4. Analysis of experimental results. Comparison with theoretical calculations

Work [2] presents a discussion on the energy stored in metal (monocrystal and polycrystal) under the assumption that deformations are small. An elastic-plastic rod subject to quasi-static and dynamic loadings was taken as an example to analyse the temperature field in a deformed material from the point of view of several hypotheses concerning the thermodynamic equation. An identical problem was solved in [1] for finite deformations on the basis of a theory that disregards the transverse inertial effects of the sample but takes into account its transverse expansion. On the basis of the method of characteristics, an initial-boundary value problem was solved for boundary and initial conditions which are identical to those in the experiments applied to the long samples described in the present work. Numerical data were close to those used for the samples tested in the experiments.

The calculated permanent longitudinal Δ_{11} and transverse deformations Δ_{22} (for a fixed time) of the sample under test are shown in Fig. 14 together with the corresponding strains measured on the deformed samples (the sample whose infrared radiation power distribution is shown in Fig. 9). The maximum deformations appear at the boundary of the sample under test. It is seen that the maximum deformations calculated and measured coincide. The differences between the measured and calculated deformations over the entire range of permanent strains can be explained by disregarding the term of instantaneous deformation in the constutive equation (cf. [1]). From the mathematical point of view this means that only disturbances with the velocities of elastic waves can propagate in the material under consideration. Plastic waves are nonexistent. It follows obviously from the experiments described here that, in a theoretical discussion on long dynamically deformed samples made of strain rate sensitive materials, it is necessary to take into account not only the deformation of a relaxation type but also the instantaneous deformations.

It was shown in ref. [7] on the example of small deformations of an inelastic bar striking a rigid obstacle that considerable differences may be observed between the distribution of permanent deformations along the bar axis Δ_{11}, and the experimental curves obtained in the cases of viscoplastic models or bodies which are not sensitive to the strain rates. However, the maximum values of permanent deformations at the front of the bar are identical for both types of materials.

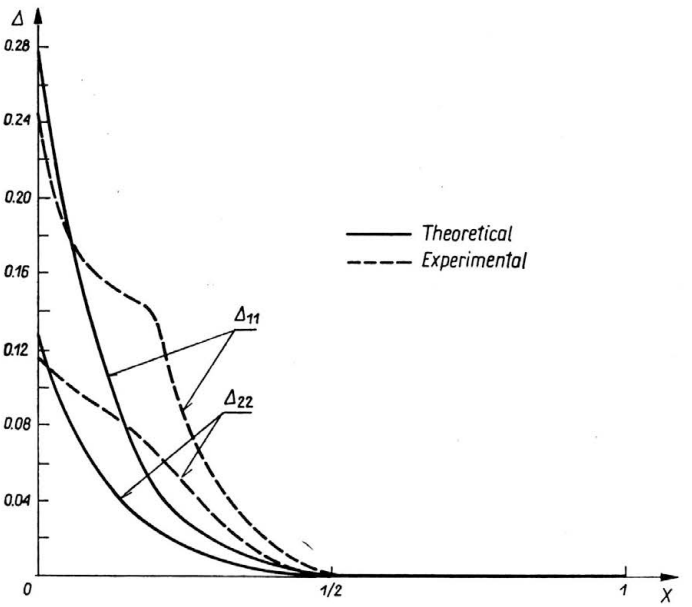

FIG. 14. Permanent deformations of sample: Δ_{11} longitudinal deformations, Δ_{22} transverse deformations, ——— calculated, - - - - - - - measured.

In [1] the term describing the instantaneous plasticity was purposely disregarded to confine the considerations to viscoelastic bodies since in such a case the numerical solution of the initial boundary value problem is much simpler than that referring to the models exhibiting instantaneous plasticity properties.

The dashed line in Fig. 15 represents the temperature variation ΔT along the sample under test (that is, along the straight line $X_1 = v_{\text{cam}}(t-t_D)$ of Fig. 7). The distribution of the power of infrared radiation along the sample is shown in Fig. 9. Temperature increase as a function of sample length was calculated on the basis of the relation H/H_w and ΔT illustrated in Fig. 2. The solid line in this figure represents the temperature increase (also along the line $X_1 = v_{\text{cam}}(t-t_D)$) calculated from the numerical solution of the initial-boundary problem considered. The impact velocity of the sample was almost identical in the two cases. The difference between the calculated and measured results can also be explained by disregarding the instantaneous plasticity in the theoretical discussion. The experimental temperature increase and the heating region of the sample face are larger than those predicted by the theory.

The experimental results are highly reproducible for both the long and short cylindrical samples. However, it is impossible to perform a more general interpretation of the results to obtain, for example, the complete relation between the temperature variation of the sample versus strain rate, permanent strains, etc. because only 30 long samples were tested in impacts against a rigid obstacle, and only 12 short cylindrical samples — in the modified Hopkinson pressure bar system. The experiments enable only a qualitative analysis of the effect and allow for the drawing conclusions on the mathematical description of dynamic deformations in the range of large strains and of the coupled equations of elasticity.

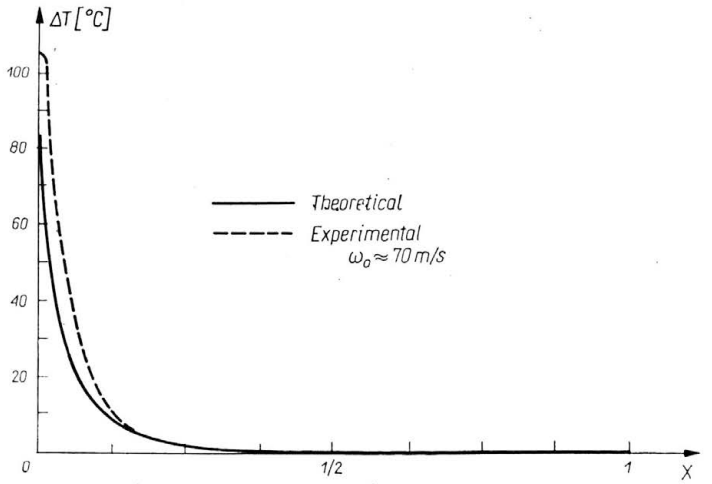

FIG. 15. Temperature increase along sample under test, on line $X_1 = v_{cam}(t - t_D)$, ——— calculated, - - - - - - - - - measured.

A number of important factors were omitted in the experiments which may prove to be of importance for the proper interpretation of the results obtained. First of all, the experiments should be performed in a vacuum, what involves serious technical difficulties in the case of dynamic deformation of the specimen. The variation of emmisivity of the surface in the process of deformation should also be taken into account; large deformations of the specimen lead to considerable deformation of its surface.

Reference

1. W. K. NOWACKI, T. KURCYK, *Sur le champ des températures en thermoélastoviscoplasticité finie*, J. Mécanique Appl. et Théoret., **1**, 4, 1982.
2. W. K. NOWACKI, J. ZARKA, *Sur le champ des températures obtenues en thermoélastoviscoplasticité*, Arch. Mech. Stos., **26**, 4, 701–715, 1974.
3. J. KLEPACZKO, *Modified Hopkinson pressure bar*, Mech. Teoret. Stos., **9**, 4, 1971 [in Polish].
4. J. A. CHARLES, F. APPL, J. E. FRANCIS, *Thermographic determination of fatigue damage*, Trans. ASME, 100, 1978.
5. C. SAIX, *Plasticité expérimentale par thermographie de surface*, Université de Montpellier, Dissertation for doctor's degree, 1978.

6. S. P. GADAJ, E. GAŁKOWSKA, J. KACZMAREK, W. OLIFERUK, *Determination of energy stored in metal during its tensioning*, IFTR Reports No 36, 1981 [in Polish].
7. H. KOLSKY, L. S. DOUCH, *Experimental studies in plastic wave propagation*, IFTR Reports No 36, 1961.
8. J. ZARKA, J. CASIER, J. J. ENGEL, *Influence de la température sur le comportement mécanique des aciers*, Industrie Minérale, March 15, 1977.
9. P. PERZYNA, *Thermodynamics of inelastic materials*, Warszawa 1978 [in Polish].
10. A. CAGNASSO, G. CANEVERT, Y. JULLIEN, R. AMALRIC, *Application de la thermovision à la mécanique vibratoire: vibrations de membranes et de plaques*, Revue d'Acoustique, 9, 1977.

POLISH ACADEMY OF SCIENCES
INSTITUTE OF FUNDAMENTAL TECHNOLOGICAL RESEARCH.

Received January 26, 1983.